Autophagy

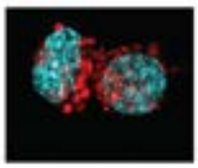

Autophagy

ISSN: 1554-8627 (Print) 1554-8635 (Online) Journal homepage: www.tandfonline.com/journals/kaup20

NMN/NAD$^+$ enhances SIRT2-modulated microtubule dynamics to improve mitochondrial and mitophagy functions in senescent cells

Jie Cui , Shifeng Ren , Bingjie Wang , Nan Zhang , Shanshan Zhu , Yajun Zhang , Xiangqing Qi , Weixue Meng , Liwei Shao , Shan Gao , Lijie Xing , Zengjun Li & Xiaodong Mu

To cite this article: Jie Cui , Shifeng Ren , Bingjie Wang , Nan Zhang , Shanshan Zhu , Yajun Zhang , Xiangqing Qi , Weixue Meng , Liwei Shao , Shan Gao , Lijie Xing , Zengjun Li & Xiaodong Mu (24 May 2026): NMN/NAD$^+$ enhances SIRT2-modulated microtubule dynamics to improve mitochondrial and mitophagy functions in senescent cells, Autophagy, DOI: 10.1080/15548627.2026.2677181

To link to this article: https://doi.org/10.1080/15548627.2026.2677181

AUTOPHAGY
https://doi.org/10.1080/15548627.2026.2677181

Taylor & Francis
by informa

RESEARCH PAPER

NMN/NAD$^+$ enhances SIRT2-modulated microtubule dynamics to improve mitochondrial and mitophagy functions in senescent cells

Jie Cui[a*], Shifeng Ren[a*], Bingjie Wang[a*], Nan Zhang[a], Shanshan Zhu[a], Yajun Zhang[a], Xiangqing Qi[a], Weixue Meng[a], Liwei Shao[a], Shan Gao[a], Lijie Xing[b], Zengjun Li[b], and Xiaodong Mu[a]

[a]School of Pharmaceutical Sciences, National Key Laboratory of Advanced Drug Delivery System, Shandong First Medical University & Shandong Academy of Medical Sciences, Jinan, China; [b]Shandong Cancer Hospital and Institute, Shandong First Medical University & Shandong Academy of Medical Sciences, Jinan, China

ABSTRACT

The effect of NAD$^+$ in enhancing mitochondrial function and energy metabolism in human cells is closely linked to NAD$^+$-dependent sirtuins (i.e. SIRT1 and SIRT3). SIRT2 primarily functions in the cytoplasm, where it can serve as a key deacetylase for tubulin and modulates stability of microtubules. Microtubule plays a pivotal role in regulating mitochondrial dynamics, including mitochondrial movement, fission/fusion, repair, and mitophagy-dependent clearance. However, the potential role of NAD$^+$ in modulating SIRT2-related microtubule stability, and the potential involvement of the NAD$^+$-SIRT2-microtubule axis in regulating mitochondrial and mitophagy functions remains unexplored. In this study, we demonstrate that senescent muscle cells exhibit microtubule hyper-stabilization and reduced dynamics, concomitant with SIRT2 inactivation and tubulin hyperacetylation. These alterations impair microtubule-dependent mitochondrial repair and mitophagy function, resulting in mtDNA leakage, CGAS-STING1 activation and subsequently accelerated senescence. Notably, treatment with nicotinamide mononucleotide (NMN) effectively reactivates SIRT2, restores microtubule dynamics, and enhances mitochondrial quality control by promoting repair and mitophagy. Consequently, NMN mitigates CGAS-STING1-driven senescence. Our findings reveal a novel mechanism by which NMN preserves mitochondrial health in senescent cells via a SIRT2-microtubule axis, highlighting its protective role beyond canonical NAD$^+$-sirtuin pathways, and suggesting microtubule dynamics as a promising therapeutic target for improving cellular defects associated with mitochondrial and mitophagy dysfunctions.

ARTICLE HISTORY
Received 12 June 2025
Revised 9 May 2026
Accepted 15 May 2026

KEYWORDS
Cellular senescence; cytoskeleton; innate immunity; mechanical stress; mitochondrial damage; mitophagy dysfunction

Abbreviations: D-gal: D-galactose; EdU: 5-ethynyl-20-deoxyuridine; HDAC6: histone deacetylase 6; LAMP1: lysosome associated membrane protein 1; MSCs: mesenchymal stem/stromal cells; mtDNA: mitochondrial DNA; NAD$^+$: nicotinamide adenine dinucleotide; NMN: nicotinamide mononucleotide; PBS: phosphate-buffered saline; SA-GLB1/β-gal: senescence-associated galactosidase beta 1; SIRT2: sirtuin 2.

Introduction

Nicotinamide mononucleotide (NMN) is a precursor of nicotinamide adenine dinucleotide (NAD$^+$), a critical coenzyme involved in various cellular processes, such as mitochondrial homeostasis, energy metabolism and DNA repair [1,2]. The potential beneficial effects of NMN/NAD$^+$ in delaying the senescence of various types of cells have been extensively studied, and the underlying mechanisms have been greatly attributed to the enhancement of mitochondrial function and improvement of energy metabolism [3,4]. NAD$^+$ levels in human cells decline with age, leading to reduced activity of NAD$^+$-dependent enzymes, including sirtuins [5]. Sirtuins are a class of NAD$^+$-dependent deacetylases that can function by removing acetyl groups from target proteins (deacetylation) and regulate gene expression, metabolism, and stress responses [5,6]. Among various target proteins of NAD$^+$, sirtuins are well-recognized for their crucial roles in lifespan extension and slowing down aging in various organisms [7,8] Particularly, SIRT2 is a unique member of the sirtuins, primarily localized in the cytoplasm, with TUBA/α-tubulin being one of its key targets of deacetylation activity [9]. Thus, SIRT2 play a critical role in influencing microtubule stability and dynamics [10]. Like other sirtuins, activity of SIRT2 also declines during cellular senescence [11]. Recent studies have shown that NMN supplementation to human cells or animal models can boost NAD$^+$ levels, improving sirtuins activity and relevant cell functions [12,13]. However, the potential effect of NAD$^+$ on the SIRT2-microtubule system, and their

CONTACT Lijie Xing xiaopiao423@126.com Shandong Cancer Hospital and Institute, Shandong First Medical University & Shandong Academy of Medical Sciences, Jinan 250117, China; Zengjun Li zjli8692@sdfmu.edu.cn Shandong Cancer Hospital and Institute, Shandong First Medical University & Shandong Academy of Medical Sciences, Jinan 250117, China; Xiaodong Mu muxiaodong@sdfmu.edu.cn School of Pharmaceutical Sciences, National Key Laboratory of Advanced Drug Delivery System, Shandong First Medical University & Shandong Academy of Medical Sciences, Jinan 250117, China
*These authors contributed equally to this study.

Supplemental data for this article can be accessed online at https://doi.org/10.1080/15548627.2026.2677181

potential role in the regulation of aging process remain unknown [13].

Cytoskeleton is the key structural element determining the mechanical properties of cells, and mechanical stress from the extracellular matrix (ECM) can be transmitted to the nucleus through cytoskeleton, and change the gene expression profile [14,15]. In addition, ECM-derived peptides can also act as ligands to activate signaling pathways and regulate (e.g., activate or inhibit) the activity of enzymes such as SIRT2, thereby altering the acetylation status and stability of the cytoskeleton [16]. Microtubule is the main cytoskeletal structure that plays an important role in regulating cell morphology or shape, cell migration or motility, cell division, nuclear deformation, signal transduction and many other cell events [17,18]. Importantly, microtubule also serves as the trafficking track for various intracellular organelles, and is critical for regulating their distribution, migration, and interaction [18]. For example, organelles such as mitochondria, autophagosomes, and lysosomes move and interact with other organelles in the cytoplasm using microtubule as guiding tracks [19]. Particularly, SIRT2 is a unique member of the sirtuins, primarily. Also, newly formed autophagosomes is transported along microtubule tracks to the peri-nuclear microtubule-organizing center (MTOC) for further processing, including its maturation and autophagosome – lysosome fusion event [20,21]. Specifically, microtubule has been demonstrated as the essential regulator of mitochondrial dynamics (i.e., fission, fusion, and motility) and repair process [22,23]. Microtubules are assembled by TUBA and TUBB/β-tubulin heterodimers, and tubulin acetylation is crucial in determining the stability of microtubule, and in regulating microtubule organization and intracellular transport. The dynamic instability of microtubule network (i.e., the polymerization and depolymerization process) is of particular importance for the kinetic activity of microtubule, which underlies their important biological functions such as the regulation of mitochondrial dynamics [24].

Recent research has indicated in many types of cells that microtubule stabilization [11] intensifies with cellular senescence [25,26], resulting in diminished microtubule dynamics and impaired microtubule-relevant cellular functions. However, how the biological functions of microtubule networks change during cellular senescence process remain much unknown. The critical role of NMN/NAD^+ on SIRT2-mediated microtubule dynamics and the potential contribution of this pathway in delaying cellular senescence deserve further investigation. Here our results support that, the enhanced SIRT2 activity by NMN/NAD^+ can lead to increased deacetylation of TUBA and improved microtubule dynamics in senescent cells, and subsequently improve mitochondrial functions that are greatly dependent on microtubule dynamics.

Therefore, in the current study, with human muscle cells as a model, we explored a potential novel mechanism of NMN-mediated anti-aging effect involving SIRT2-microtubule axis, and will clarify whether NMN can delay muscle cell senescence by activating SIRT2-modulated microtubule dynamics. Results of this study can improve our understanding of the mechanism of effective anti-aging strategies such as NMN or other anti-aging drugs, and will find out the potential therapeutic value of microtubule-targeting methods in addressing age-related muscle degeneration and sarcopenia disease.

Results

NMN effectively delayed muscle cell senescence

We established a cellular senescence model using D-galactose (D-gal)-treated human skeletal muscle-derived MSCs [27,28]. Then the senescent MSCs were treated with NMN of varied concentrations (0, 50, 70, 100 and 150 μM) for 3 days. Results showed that NMN of 100 μM was most effective in reducing the ratio of senescent cells, as evidenced by SA-GLB1/β-Gal staining (Figure 1A). Further validation using fluorescent staining of SA-GLB1/β-Gal (CellEvent Senescence Green) and EdU assays demonstrated reduced senescence markers and enhanced proliferation in NMN-treated cells (Figure 1B, C). The initial experiments to verify the cellular senescence model was performed by testing the cytotoxic effects of varying D-gal concentrations (20, 30, and 40 g/L) over 3 days, and 30 g/L of D-gal was identified as optimal for inducing senescence without significant cell death (Figure S1A-B). Western blot (CDKN2A/p16, CDKN1A/p21) and PCR (*CDKN2A*, *CDKN1A*, and senescence-associated secretory phenotype (SASP) factors *CXCL1, MMP1, IL1A/IL-1α, IL1B/IL-1β*, and *IL6*) analyses confirmed senescence induction (Figure S1C-D).

Furthermore, in MSCs isolated from naturally aged mice, extended NMN treatment (100 μM, 7 days) also led to a notable reduction in the number of SA-GLB1/β-Gal-positive cells compared with the untreated group, despite the presence of replicative senescence (Figure S2). This suggests that NMN can, to some extent, delay the rate of cellular senescence, though it does not significantly reverse the established senescent phenotype.

NMN led to re-activation of SIRT2 and relieved microtubule hyper-stabilization in senescent muscle cells

Our previous finding revealed increased cytoskeleton stiffness and disorganization in progeria aged cells [18,29], and it was shown in others' studies that microtubules in senescent cell develop abnormal structure and organization [11]. A dynamic microtubule network with smooth polymerization and depolymerization activities is important for proper microtubule functions, especially for its roles in modulating the distribution and movement of intracellular organelles and vesicles [30,31].

Here we found that D-gal-induced senescent muscle cells exhibited disorganized microtubules, characterized by increased polymerization, shortened length, and excessive curvature (Figure 2A-B). Meanwhile, the microtubule polymerization assay by turbidity measurement method also supports that D-gal induced increased microtubule polymerization in muscle cells (Figure S3). This result suggests that there is increased microtubule hyper-stabilization and decreased microtubule dynamics in D-gal induced

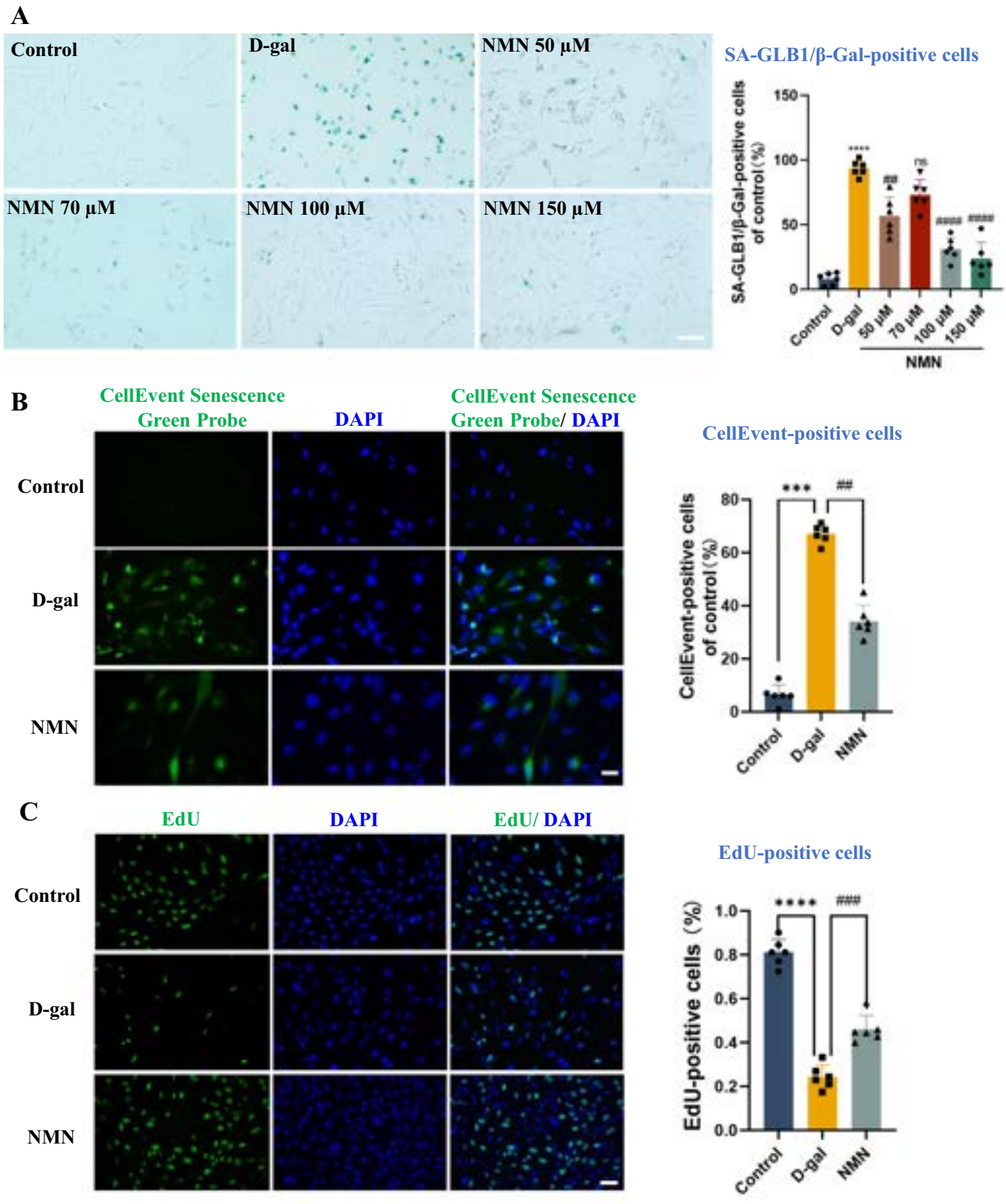

Figure 1. NMN delayed cellular senescence of human muscle MSCs. (a) After treatment of human muscle MSCs with different concentrations of NMN, the number of SA-GLB1/β-gal-positive cells and the number of senescent cells were statistically analyzed under a microscope. Scale bar: 100 μm. Data are presented as mean ± sd ($n = 6$). Unpaired Student's t-test was used for statistical analysis. Compared with control, ****$p < .0001$. And compared with D-gal group, ns $p > 0.05$, ##$p < .01$, ####$p < .0001$. (b) After treatment of human muscle MSCs with NMN (100 μM, 3 days), the number of CellEvent-positive cells were observed under a fluorescence microscope. Aging cells showed green fluorescence and the nuclei were blue. Scale bar: 100 μm. Data are presented as mean ± sd ($n = 6$). Unpaired Student's t-test was used for statistical analysis. Compared with control, ***$p < .001$. And compared with D-gal group, ##$p < .01$. (C) After treatment of human muscle MSCs with NMN, EdU measurement was performed, and the number of EdU-positive cells (green) and Hoechst-stained nucleus of all the cells (blue) were observed under a fluorescence microscope, along with a statistical chart of EdU-positive cells. Scale bar: 100 μm. Data are presented as mean ± sd ($n = 6$). Unpaired Student's t-test was used for statistical analysis. Compared with control, ****$p < .0001$. And compared with D-gal group, ###$p < .001$.

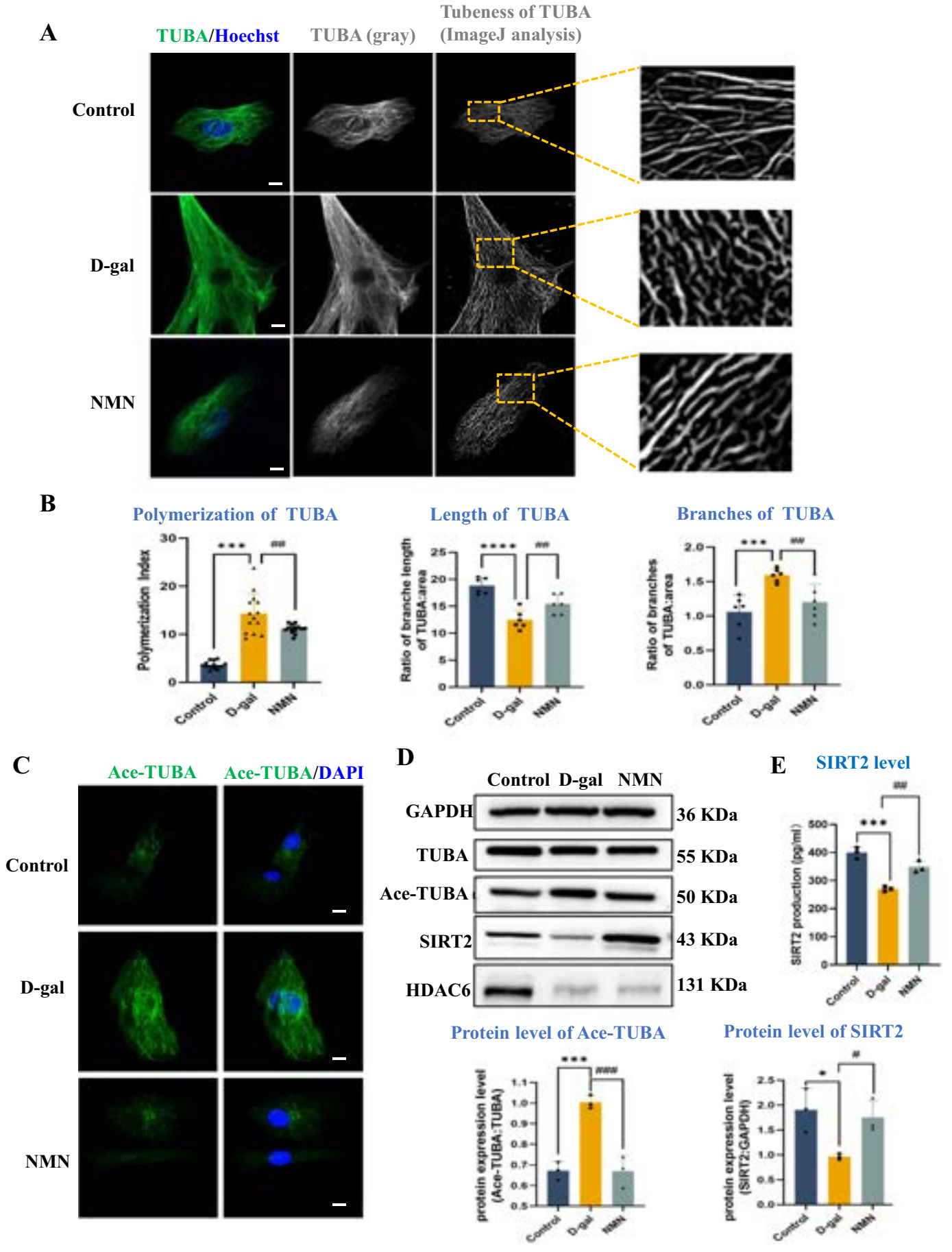

Figure 2. NMN relieved microtubule hyper-stabilization in senescent muscle cells. (a) NMN changed organization/structure of microtubule network in senescent muscle cells. The microtubule is fluorescent green and the nuclei are labelled by Hoechst (blue). The microtubule images were transferred to gray by ImageJ and then tubeness plugin was used to discern "linear" polymerized microtube. Scale bar: 10 μm. (b) the statistical analysis of microtubule status in (a). Polymerization of TUBA,

senescent muscle cells. The status of microtubule polymerization is closely related to the level of TUBA acetylation [32], and here our result showed that senescent muscle cells had elevated level of TUBA acetylation (Figure 2C-D). Meanwhile, the protein level of the two most important tubulin deacetylases HDAC6 and SIRT2, was found to be greatly reduced in senescent muscle cells (Figure 2C-D). Furthermore, direct measurement of SIRT2 deacetylase activity confirmed its significant reduction in senescent muscle cells (Figure 2E). Thus, the elevated TUBA acetylation and decreased microtubule dynamics in senescent muscle cells can be mediated by deactivation of HDAC6 and SIRT2.

Microtubule network has important roles in maintaining normal cell functions, and develops profound changes during cellular senescence [25,33]. Since NMN is able to delay the senescence of muscle MSCs, here we examined potential impact of NMN treatment on microtubule network in senescent cells (Figure 2A-B). We found that NMN treatment of senescent muscle cells led to obvious changes in microtubule network, including reduced microtubule polymerization index, and restored linear arrangement and polarity distribution (Figure 2A-B). Also, immuno-fluorescent staining of acetylated TUBA showed that NMN reduced the level of TUBA acetylation, suggesting that it might repress microtubule hyper-stabilization by increasing TUBA de-acetylation (Figure 2C-D). Sirtuins (including SIRT2) are NAD^+-dependent deacetylase, and our western blot results showed that, NMN treatment of senescent muscle cells significantly increased the level of SIRT2 protein (but not HDAC6) (Figure 2C-E), which can be responsible for the reduced level of TUBA acetylation.

NMN-induced destabilization of microtubules in senescent cells improved mitochondrial repair and function

Previous studies on NMN have primarily focused on its direct effects on mitochondrial characteristics and functions, such as modulating oxidative phosphorylation, mitigating oxidative stress, and improving energy metabolism. However, the functions and dynamics of mitochondria is intricately linked to the status of microtubule, which serve as the primary cytoskeletal structures regulating multiple critical cellular processes [34]. In particular, microtubule acts as intracellular transport/trafficking tracks for various types of organelles including mitochondria, orchestrating their distribution, motility, fusion, fission, and repair, as well as the mitophagy process [35,36]. Thus, we hypothesized that dysfunction in microtubule networks could exacerbate mitochondrial damage and interfere with the mitochondrial repair mechanisms, and that NMN might reverse these defects.

Here our results showed that, hyper-stabilized microtubule network in senescent muscle cells is coupled with increased level of fragmented mitochondria (Figure 3A-B), while NMN treatment (100 μM, 3 days) effectively restored mitochondrial morphology (length, branching, and network integrity) and function, evidenced by increased NAD^+: NADH ratios, ATP production, and reduced lactate accumulation (Figure S4A – C). Additionally, NMN restored mitochondrial membrane potential, reduced oxidative stress (mitoSOX), and decreased the level of oxidative damage to mitochondrial DNA (mtDNA), as evidenced by immunostaining of 8-OHdG (Figure S4D).

Next, in order to further verify that the improvement of mitochondrial functions by NMN can be mediated by SIRT2-microtubule axis, we used plasmid vectors carrying DNA fragments encoding SIRT2-GFP to re-activate the TUBA deacetylase activity of SIRT2. Result showed that, SIRT2 overexpression in senescent muscle cells produced similar results as NMN treatment, including decreased level of microtubule hyper-stabilization, improved mitochondrial morphology and reduced mitochondrial damage (Figures 3, 4). Meanwhile, transient microtubule depolymerization in senescent muscle cells by low-dose of microtubule depolymerizer colchicine (2 nM, 3 days) was also effective in relaxing hyper-stabilized microtubule network and reducing mitochondrial damage (Figures 3, 4), which result is consistent with previous observations of colchicine's effect in repressing ROS, inflammation, autophagy, and senescence [37–39].

Collectively, these findings demonstrate that SIRT2-microtubule axis plays a critical role in mediating the effect of NMN on mitochondrial/ functions, and that NMN's restoration of microtubule dynamics is possibly indispensable for rescuing mitochondrial function in senescent cells. By improving microtubule-dependent mitochondrial trafficking and dynamics, NMN could mitigate metabolic dysfunction and oxidative stress in mitochondria, underscoring the cytoskeleton's pivotal role in mediating its anti-aging effects.

NMN reduced mtDNA leakage and CGAS-STING1 activation through restoring microtubule dynamics

Usually, DNA in cells is strictly contained in the nucleus or mitochondria, and the presence of DNA in the cytoplasm is a danger signal to cells. Just like DNA from viral or bacterial infection, DNA leaked from damaged mitochondria can activate the innate immune response of cells, especially the CGAS-STING1 signal [40]. Our previous research has revealed that increased mitochondrial damage can lead to increased mtDNA

ratio of aggregated microtubules area:cell area, indicated the degree of microtubule aggregation. The tubeness images were then analyzed with ImageJ mitochondrial network analysis (MiNA) toolset plugin to check structural changes of microtubule. With this plugin, we analyzed and compared changes in microtubule branches (number of microtubule branches) and branch junctions (crossing of microtubule filament). Our result showed NMN improve D-gal-induced disordered microtubule network, including reduced microtubule aggregation, restored linear arrangement and polarity distribution ($n = 6$). Unpaired Student's t-test was used for statistical analysis. Compared with control, ****$p < .001$. And compared with D-gal group, ##$p < .01$, ####$p < .001$. (C) NMN decreased the level of microtubule acetylation in senescent muscle cells. Immunofluorescence staining of acetyl-TUBA (ace-TUBA, bright green). The nuclei are labelled by DAPI (blue). Scale bar: 10 μm. (d) Western blot was used to detect the expression levels of ace-TUBA, the microtubule histone deacetylase HDAC6 and SIRT2 after NMN treatment. Statistical analysis was performed for western blot result, and are presented as mean ± sd ($n = 3$). Unpaired Student's t-test was used for statistical analysis. Compared with control, ***$p < .05$, ##$p < .001$. And compared with D-gal group, ****$p < .05$, ###$p < .001$. (e) the activity of SIRT2 was determined with an Elisa kit by measuring the absorbance at 450 nm (OD_{450}) of lysates from 1×10^6 cells. Data are presented as mean ± sd ($n = 3$). Unpaired Student's t-test was used for statistical analysis. Compared with control, **$p < .001$. And compared with D-gal group, #$p < .01$.

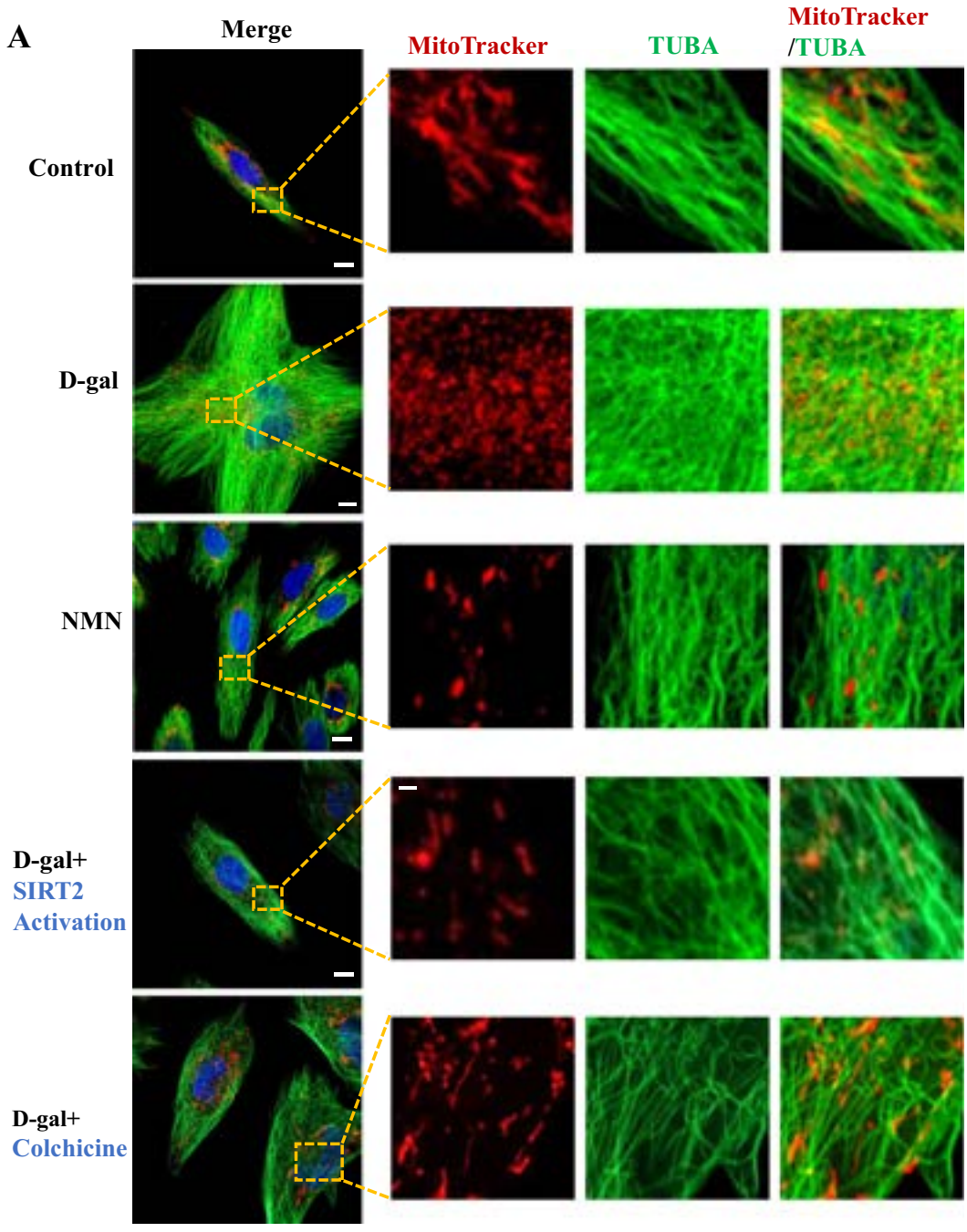

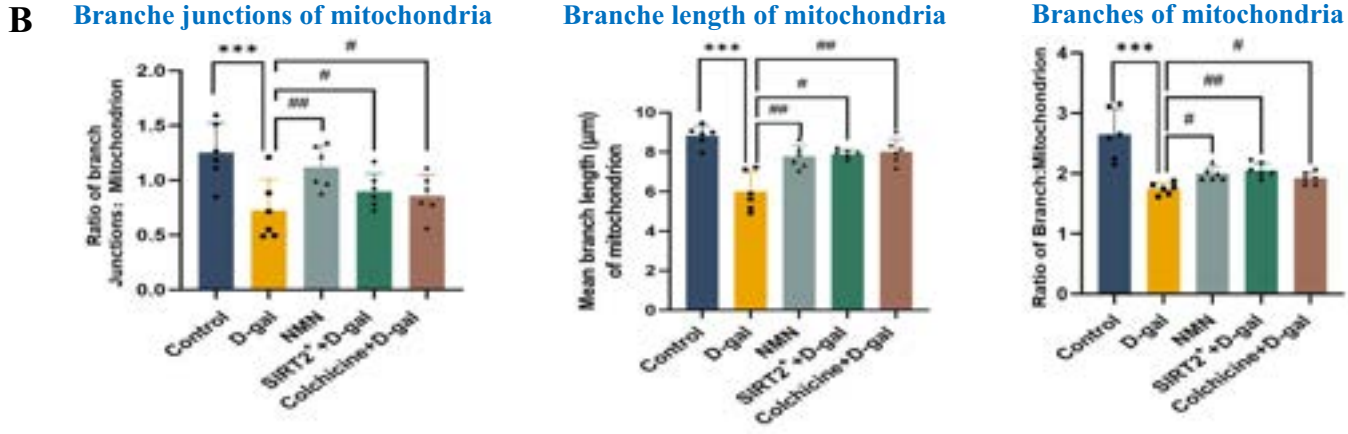

Figure 3. NMN-induced destabilization of microtubules in senescent cells restored abnormal mitochondrial morphology and distribution. (a) confocal imaging showing NMN and microtubule destabilization (SIRT2 over expression and colchicine, 2 nM, 3 days) effectively improve mitochondrial distribution in senescent cells. vital cell staining of mitochondria (MitoTracker, red) and microtubule (green). The nuclei are labelled by Hoechst (blue). Scale bar: 10 μm. (b) mitochondrial morphology analysis. Mitochondria analyzer plugin in ImageJ was used for mitochondrial morphological analysis. Scale bar: 10 μm. Data are presented as mean ± sd ($n = 6$). Unpaired Student's t-test was used for statistical analysis. Compared with control, ****$p < .001$. And compared with D-gal group, ##$p < .05$, ####$p < .01$.

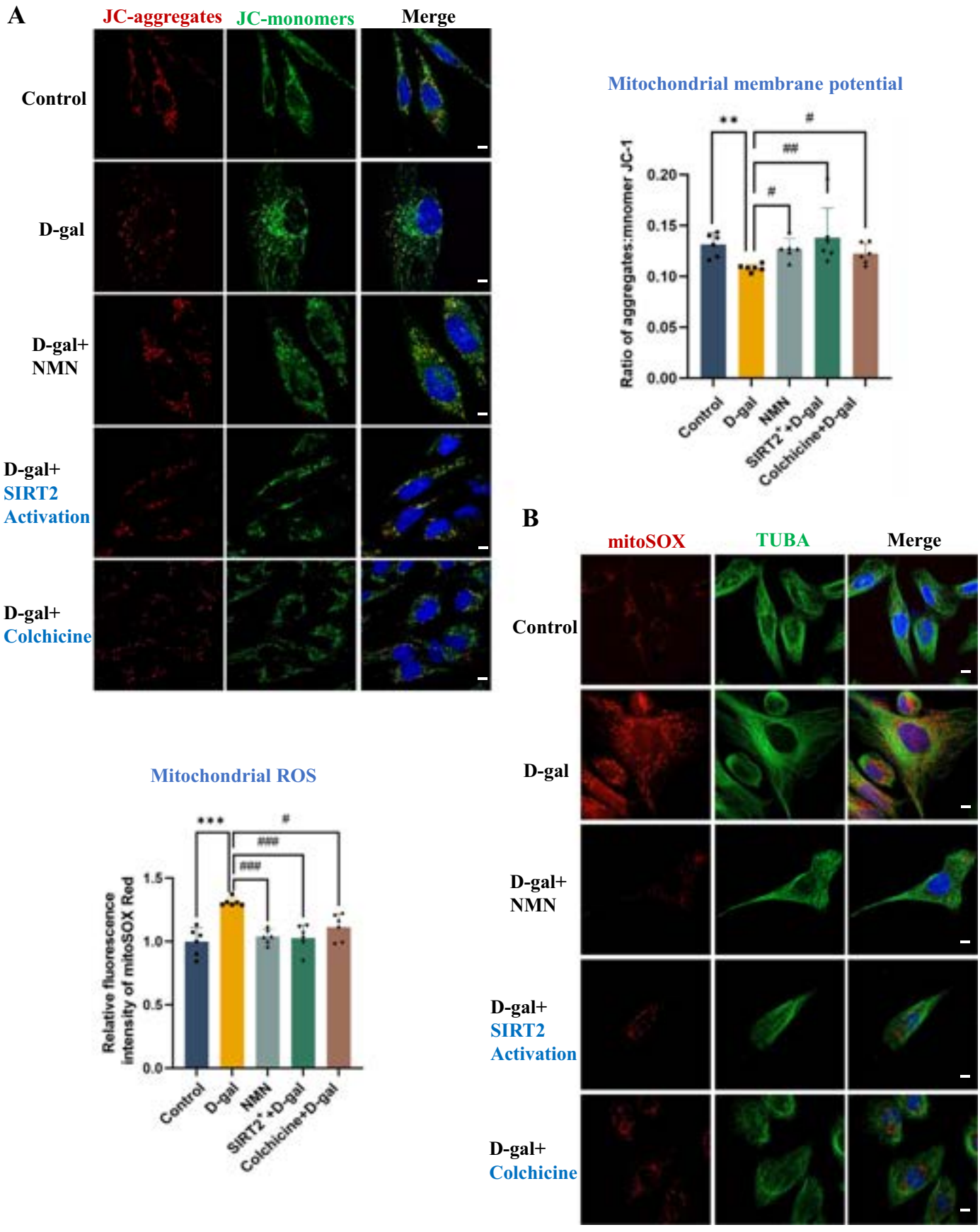

Figure 4. NMN-induced destabilization of microtubules in senescent cells restored mitochondrial function. (a) Confocal imaging of changes after NMN and microtubule destabilization (SIRT2 overexpression and colchicine) treatment in the mitochondrial membrane potential stained by JC-1 (green: J-monomers in low-potential; red: J-aggregates in healthy high-potential). Statistics was done to the ratio of fluorescence red to green, to indicate the level of normal mitochondrial membrane potential. Scale bar: 10 μm. Data are presented as mean ± sd ($n = 6$). Unpaired Student's t-test was used for statistical analysis. Compared with control, ****$p < .01$. And compared with D-gal group, ##$p < .05$, ####$p < .01$. (b) mtROS level were examined by mitoSOX indicator (red). Scale bar: 10 μm. Data are presented as mean ± sd ($n = 6$ visions). Unpaired Student's t-test was used for statistical analysis. Compared with control, ***$p < .001$. And compared with D-gal group, ##$p < .05$, ****$p < .001$.

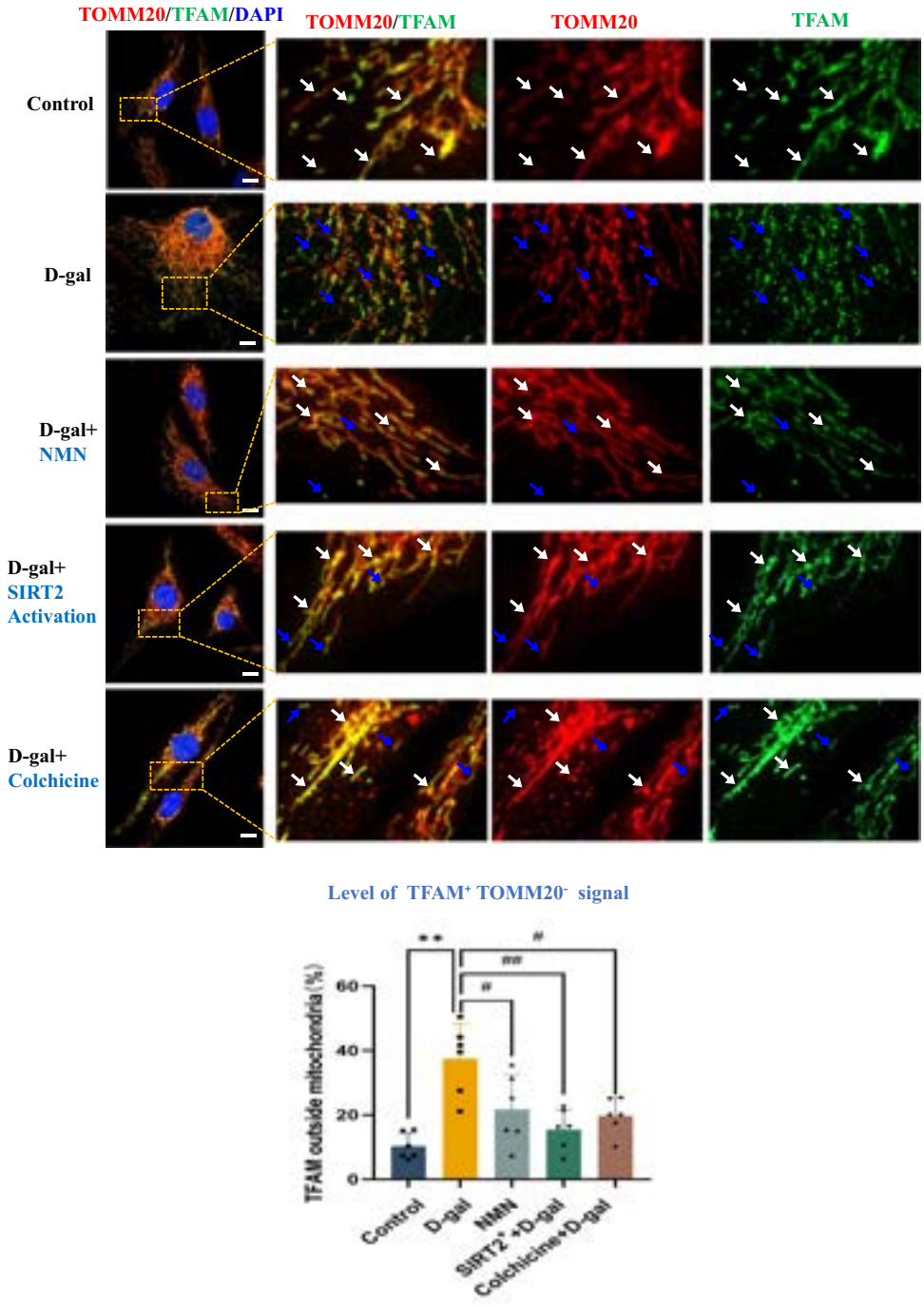

Figure 5. NMN reduced the level of mtDNA leakage in senescent muscle cells. Confocal imaging of cells after NMN and microtubule destabilization (SIRT2 over expression and colchicine) treatment for the leaked mtDNA stained by TFAM (a protein binding with DNA) and TOMM20 (a mitochondria membrane protein), mtDNA localized inside mitochondria are marked by white arrow ($TFAM^+$ $TOMM20^+$); mtDNA leaked into cytoplasm are marked by blue arrow ($TFAM^+$ $TOMM20^-$). Statistical analysis of TFAM in cytosol. Statistics was done to the ratio of fluorescence green (no overlap with red) to green (total), to indicate the level of mtDNA leakage. Scale bar: 10 μm. Data are presented as mean ± sd ($n = 6$). Unpaired Student's t-test was used for statistical analysis. Compared with control, ****$p < .01$. And compared with D-gal group, ##$p < .05$, ####$p < .01$.

leakage and activation of CGAS-STING1 in senescent myofibers [41]. Here we explored whether microtubule abnormalities have a role in mediating the mitochondrial damage-induced mtDNA leakage and CGAS-STING1 activation in senescent MSCs, and whether NMN supplementation had an impact on this process.

TFAM protein binds to mtDNA to form a nucleoid structure that protects mtDNA from damage and ensures its stability and normal function [42]. Our immunofluorescence staining results showed the presence of a large number of extra-mitochondrial TFAM in senescent muscle cells, which implies the increased leakage of mtDNA. Then, NMN treatment of the senescent muscle cells significantly reduced the level of mtDNA leakage (Figure 5). Also, the protein levels of CGAS-STING1 signaling-related factors (i.e., CGAS, STING1, p-STING1) and the gene expression level of target genes of CGAS-STING1 signaling (*IFNA/IFN-α* and *IFNB/IFN-β*), was significantly decreased (Figure 6), supporting that NMN is effective in repressing CGAS-STING1 activation.

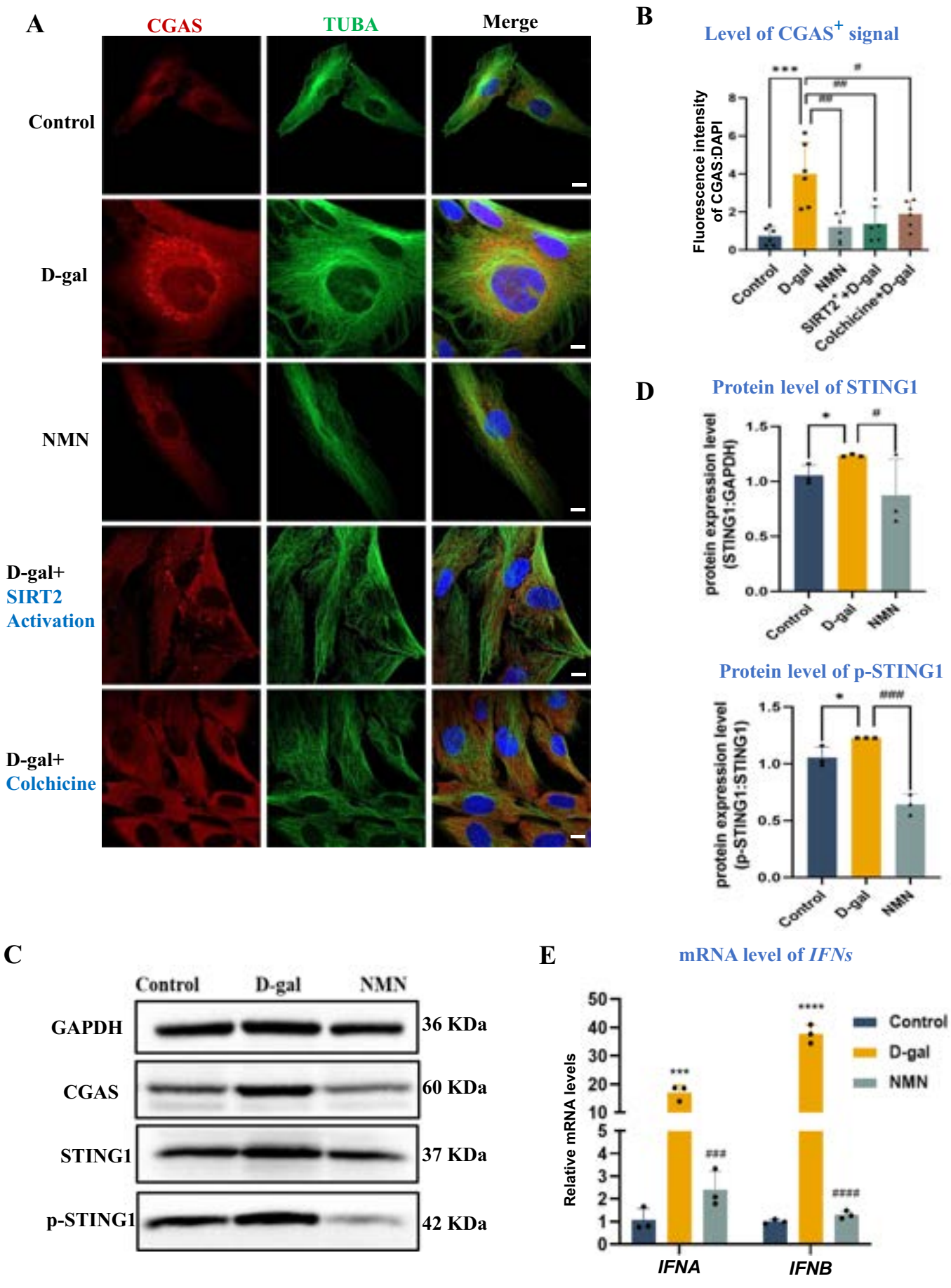

Figure 6. NMN decreased CGAS-STING1 activation in senescent muscle cells. (a) Confocal imaging of CGAS signal after NMN and microtubule destabilization (SIRT2 over expression and colchicine) treatment. Scale bar: 10 μm. (b) Statistics of a was done to the ratio of fluorescence red to green, to indicate the intensity of CGAS

Further, in order to validate the involvement of SIRT2-microtubule axis in mediating the effect of NMN in reducing mtDNA leakage and CGAS-STING1 activation, we performed SIRT2 overexpression or modulation of microtubule stability by low-dose of colchicine in senescent muscle cells. Results showed that both SIRT2 overexpression and transient microtubule depolymerization displayed similar results as NMN treatment (Figures 5, 6), supporting the significant involvement of SIRT2-microtubule axis in regulating mtDNA leakage and CGAS-STING1 activation.

Therefore, it is possible that NMN can restore the function of damaged mitochondria or speed up the clearance of damaged mitochondria by regulating the microtubule dynamics, and reduce the total number of damaged mitochondria in senescent MSCs, thereby reducing mtDNA leakage and CGAS-STING1 activation.

NMN enhanced mitophagy function in senescent muscle cells through restoring microtubule dynamics

Changes in microtubule properties can also have a significant impact on the location, movement, function, and interaction of organelles such as autophagosomes and lysosomes [43]. Autophagosomes are also a part of the innate immune system, and the clearance of aging or damaged mitochondria requires the participation of autophagosomes/lysosomes to initiate and promote mitophagy, so as to avoid the leakage of ROS and mtDNA into the cytoplasm. As shown above, we have observed a significant reduction of mitochondrial damage in senescent MSCs with NMN treatment, so we further examined the microtubule-mediated changes in mitophagy with NMN treatment.

Confocal imaging of fluorescent probes for lysosomes (LysoTracker) showed an increased accumulation of lysosomal vesicles in senescent muscle cells (Figure 7), suggesting potentially impaired lysosomal function. Consistently, immunofluorescent staining of LAMP1 (a lysosome-related protein) also showed obviously increased peri-nuclear accumulation in human senescent muscle cells (Figure S5), which is coupled with disorganized microtubule structure. Western blot assay of mitophagy-related proteins (i.e., PRKN/Parkin and PINK1) in senescent MSCs also showed that the level of PRKN and PINK1 were significantly increased (Figure 7B). Together with the observation of increased accumulation of lysosomal vesicles in the senescent cells above, the increased level of PRKN and PINK1 may indicate that damaged mitochondria or mitochondrial autophagosomes ($PINK1^+$ and $PRKN^+$) in senescent muscle cells cannot properly interact and fuse with lysosomal vesicles ($LysoTracker^+$ and $LAMP1^+$) to proceed with mitophagy-dependent degradation process smoothly. Further, NMN treatment of the human senescent muscle cells effectively reduced the accumulation of $LAMP1^+$ (Figure S5), and reversed the expression level of PRKN and PINK1 proteins (Figure 7B). To directly assess the level of mitophagy, we applied a mitophagy detection Kit with the Mtphagy Dye probe [44]. Results showed that there was a significant increase in fluorescence intensity of mitophagy in D-gal-induced senescent cells, indicating the accumulation of damaged mitochondria. While when the senescent cells were treated with NMN (100 μM, 3 days), the mitophagy flow was effectively restored (Figure S6), indicating improved lysosomal and mitophagy functions in NMN-treated senescent cells.

In order to further verify the involvement of microtubule dynamics in affecting mitophagy function, SIRT2 overexpression or transient modulation of microtubule stability by colchicine were performed in senescent muscle cells. Results showed that both SIRT2 overexpression and transient microtubule depolymerization displayed similar results as NMN treatment in reducing the extensive accumulation of lysosomal vesicles (Figure 7, Figure S5), supporting the significant involvement of SIRT2-microtubule axis in regulating mitophagy function. Moreover, studies on MSCs isolated from both young and aged mice further demonstrate that microtubule modulation may serve as an effective strategy to ameliorate lysosomal accumulation and promote mitophagy (Figure S7). To further validate the direct effect of NMN on SIRT2, we transfected human muscle cells with plasmid over-expressing *SIRT2* siRNA followed by NMN treatment. Our results demonstrated that although NMN could partially reduce the perinuclear accumulation of $LAMP1^+$ organelles after SIRT2 knockdown, its effect was significantly weaker compared to NMN treatment alone (Figure S8). We speculate that alternative or parallel pathways (such as SIRT1 or SIRT3) may exist, potentially directly improving mitochondrial function through the supplementation of cellular NAD^+ levels. Nevertheless, our results still demonstrate that SIRT2 is a key downstream pathway for NMN, and an essential mediator through which NMN modulates microtubules to ameliorate mitophagy dysfunction.

NMN improved mitochondrial and mitophagy function of muscle cells through modulating SIRT2-microtubule axis

The results above demonstrated the effect of NMN supplementation on SIRT2- mediated microtubule deacetylation and restoration of microtubule dynamics. In order to further verify that the significant involvement of SIRT2-microtubule axis in mediating the beneficial effects of NMN on senescent muscle cells, we compared the effects of SIRT2 overexpression and the SIRT2 selective inhibitor SirReal2, and also compared the effects of direct regulators of microtubule polymerization and depolymerization.

signal. Data are presented as mean ± sd ($n = 6$). Unpaired Student's t-test was used for statistical analysis. Compared with control, ****$p < .001$. And compared with D-gal group, ##$p < .05$, ####$p < .01$. (C) Western blot results showing the protein levels of CGAS-STING1 pathway factors (CGAS, STING1 and p-STING1) after NMN treatment. (d) Statistics of B. Our results showed NMN can effectively repress CGAS-STING1 activation. Data are presented as mean ± sd ($n = 3$). Unpaired Student's t-test was used for statistical analysis. Compared with control, ***$p < .05$. And compared with D-gal group, ##$p < .05$, ****$p < .001$. (e) The expression level of innate immune-activated *IFNA* and *IFNB* detected by RT-qPCR. Data are presented as mean ± sd ($n = 3$). Unpaired Student's t-test was used for statistical analysis. Compared with control, ###$p < .001$, **$p < .0001$. And compared with D-gal group, #$p < .001$, ##$p < .0001$.

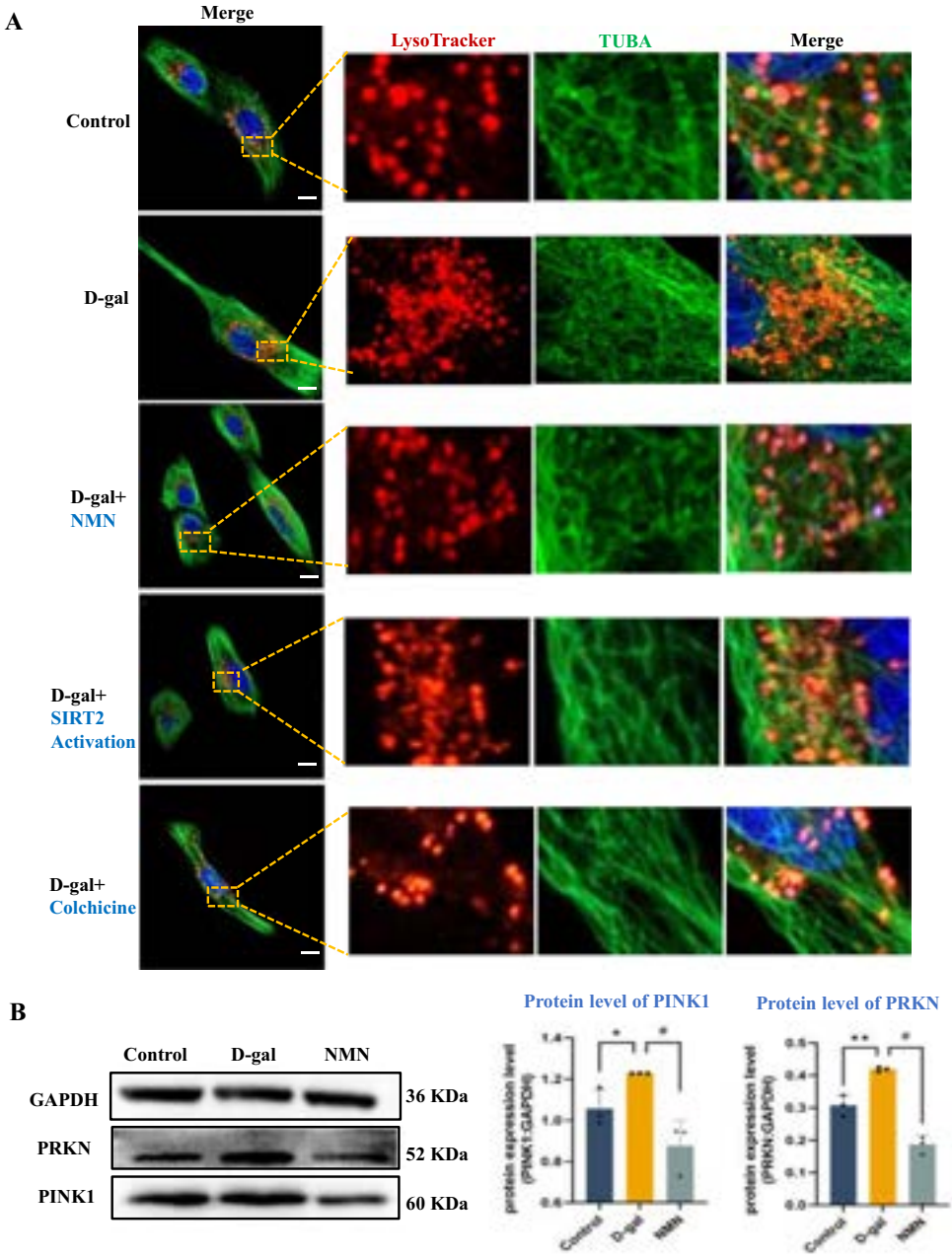

Figure 7. NMN decreased accumulation of lysosomes in senescent muscle cells. (a) Immunostaining of human muscle senescent cells after NMN and microtubule destabilization (SIRT2 over expression and colchicine) treatment revealed the differential distribution of $LAMP1^{+}$ signal (red; a marker for lysosomal and autophagosome vesicles). Statistics was done to the ratio of fluorescence red to blue. Scale bar: 10 μm. Data are presented as mean ± sd ($n = 6$). (b) Western blot results showing the protein levels of mitophagy-related factors (PRKN and PINK1) after NMN treatment. ($n = 3$). Unpaired Student's t-test was used for statistical analysis. Compared with control, ****$p < .05$, ##$p < .01$. And compared with D-gal group, ####$p < .05$.

Our results show that, SIRT2 overexpression in D-gal induced senescent muscle cells produced a similar effect of NMN supplementation, and microtubule hyperacetylation was prevented. Moreover, the expression levels of CGAS-STING1 signaling factors (i.e., CGAS, STING1 and p-STING1) and lysosome or mitophagy-related proteins (i.e., LAMP1, PRKN and PINK1) were decreased; in contrast, inhibition of SIRT2 activity by SirReal2 (5 μM, 3 days) resulted in an effect consistent with D-gal induce cellular senescence in muscle cells (Figure 8). This proves that NMN improves cell senescence by enhancing SIRT2 activity. Also, paclitaxel (5 nM, 2 days) and colchicine (2 nM, 3 days) were used individually here to promote microtubule polymerization and depolymerization. And similarly, after paclitaxel was used to stabilize microtubules in muscle cells, significant mitophagy disorders and CGAS-STING1 activation were observed, while muscle cells co-treated with D-gal and colchicine at lower concentrations showed lower level of mitophagy disorders and CGAS-STING1 activation (Figure 9). There results further support that SIRT2-micrtoubule axis is greatly involved in mediating the anti-aging effect of NMN.

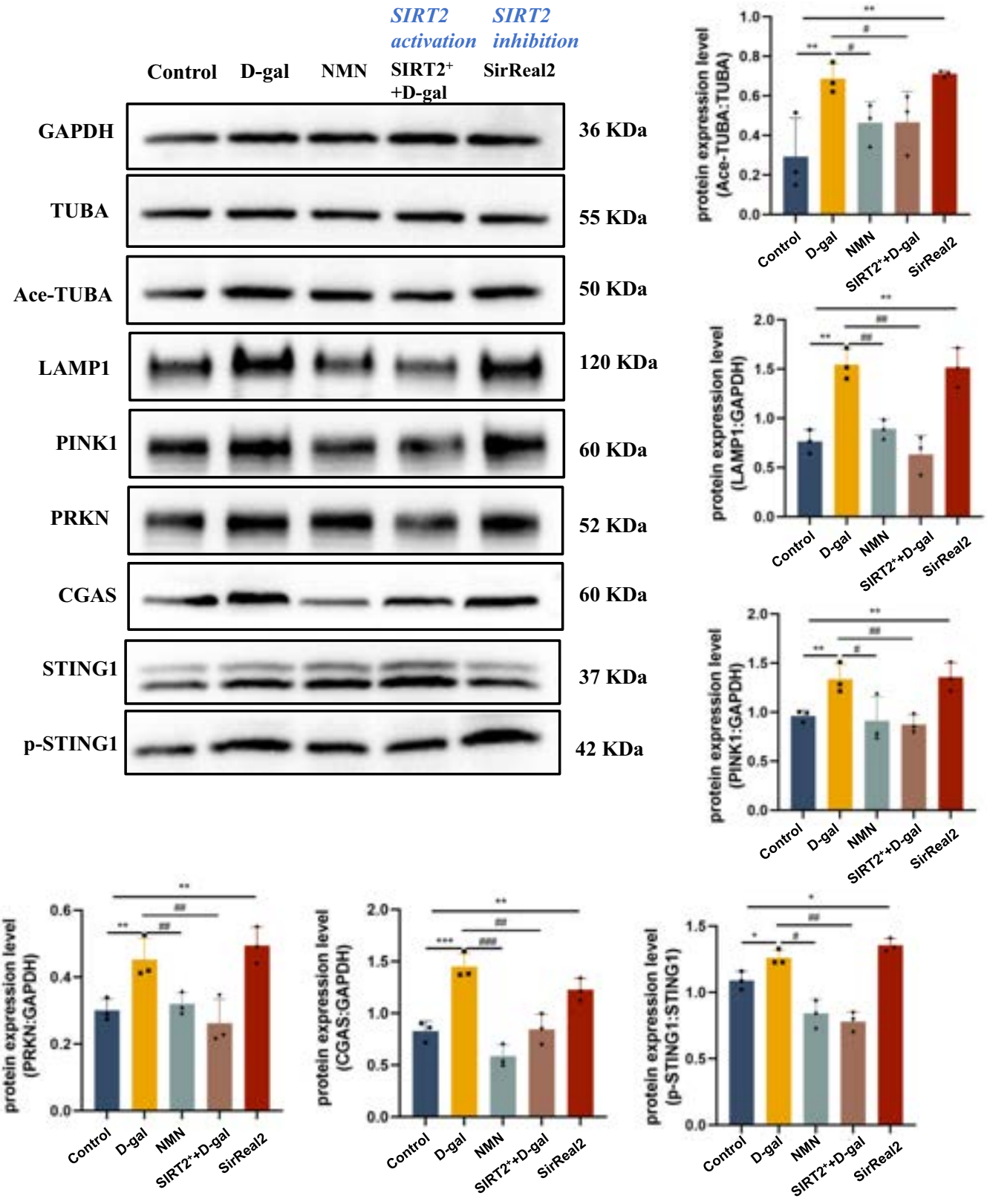

Figure 8. SIRT2 regulation changes the state of TUBA acetylation, mitophagy function and CGAS-STING1 activation. Western blot results showing the protein levels of acetylation of microtubules, mitophagy-related pathway factors (LAMP1, PRKN and PINK1) and CGAS-STING1 pathway factors (CGAS, STING1 and p-STING1) after NMN treatment, SIRT2 overexpression (*SIRT2* plasmid) and SIRT2 inhibition (SirReal2, 5 μM, 3 days). Data are presented as mean ± sd ($n = 3$). Unpaired Student's t-test was used for statistical analysis. Compared with control, ****$p < .05$, ##$p < .01$, ####$p < .001$. And compared with D-gal group, ***$p < .05$, ##$p < .01$, ****$p < .001$.

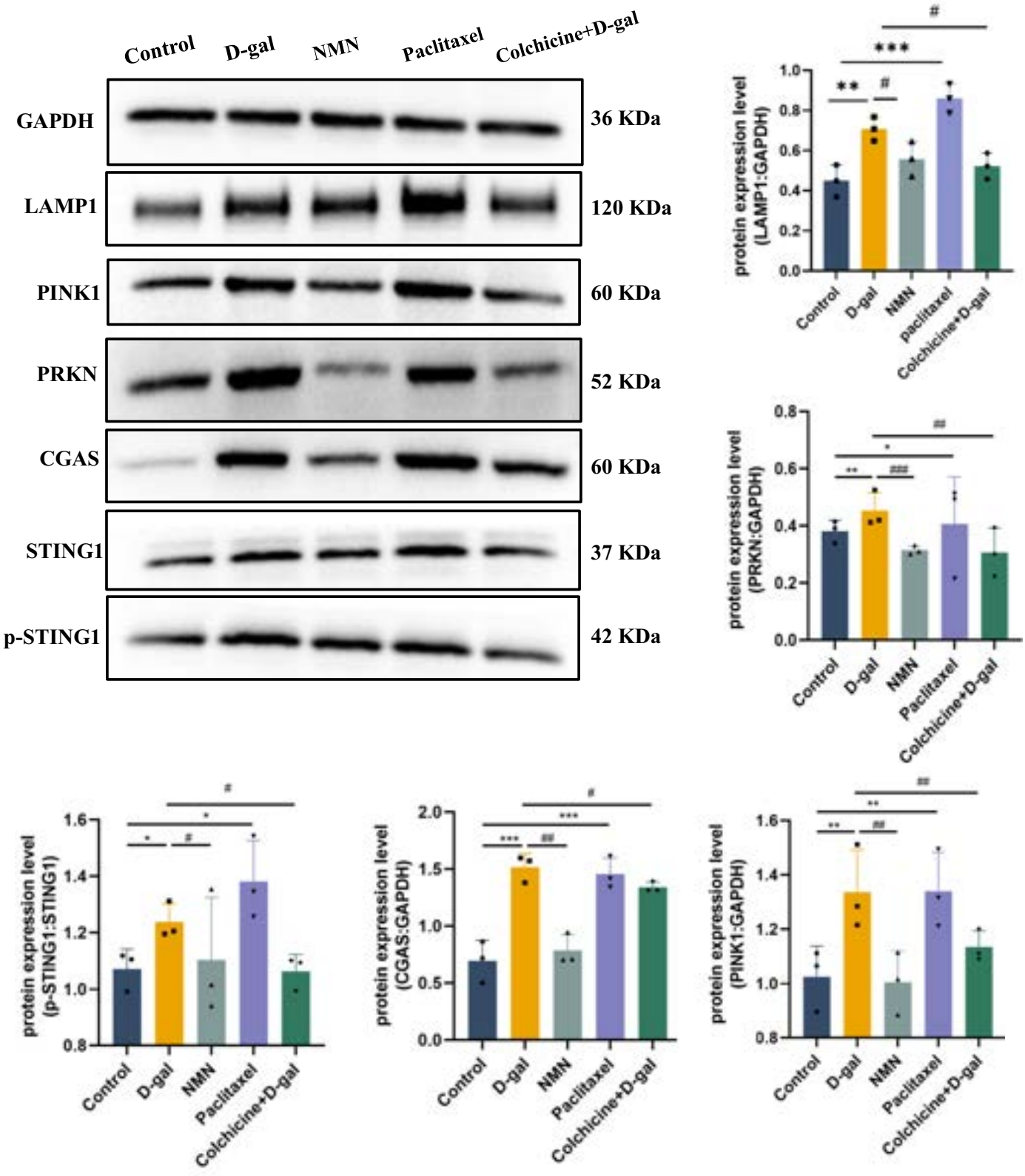

Figure 9. Microtubule polymerization/depolymerization changes the state of mitophagy function and CGAS-STING1 activation. Western blot results showing the protein levels of mitophagy-related pathway factors (LAMP1, PRKN and PINK1) and CGAS-STING1 pathway factors (CGAS, STING1 and p-STING1) after NMN treatment, microtubule aggregation (paclitaxel, 5 nM, 2 days) and depolymerization (colchicine, 2 nM, 3 days). Data are presented as mean ± sd ($n = 3$). Unpaired Student's t-test was used for statistical analysis. Compared with control, ****$p < .05$, ##$p < .01$, ####$p < .001$. And compared with D-gal group, ***$p < .05$, ##$p < .01$, ****$p < .001$.

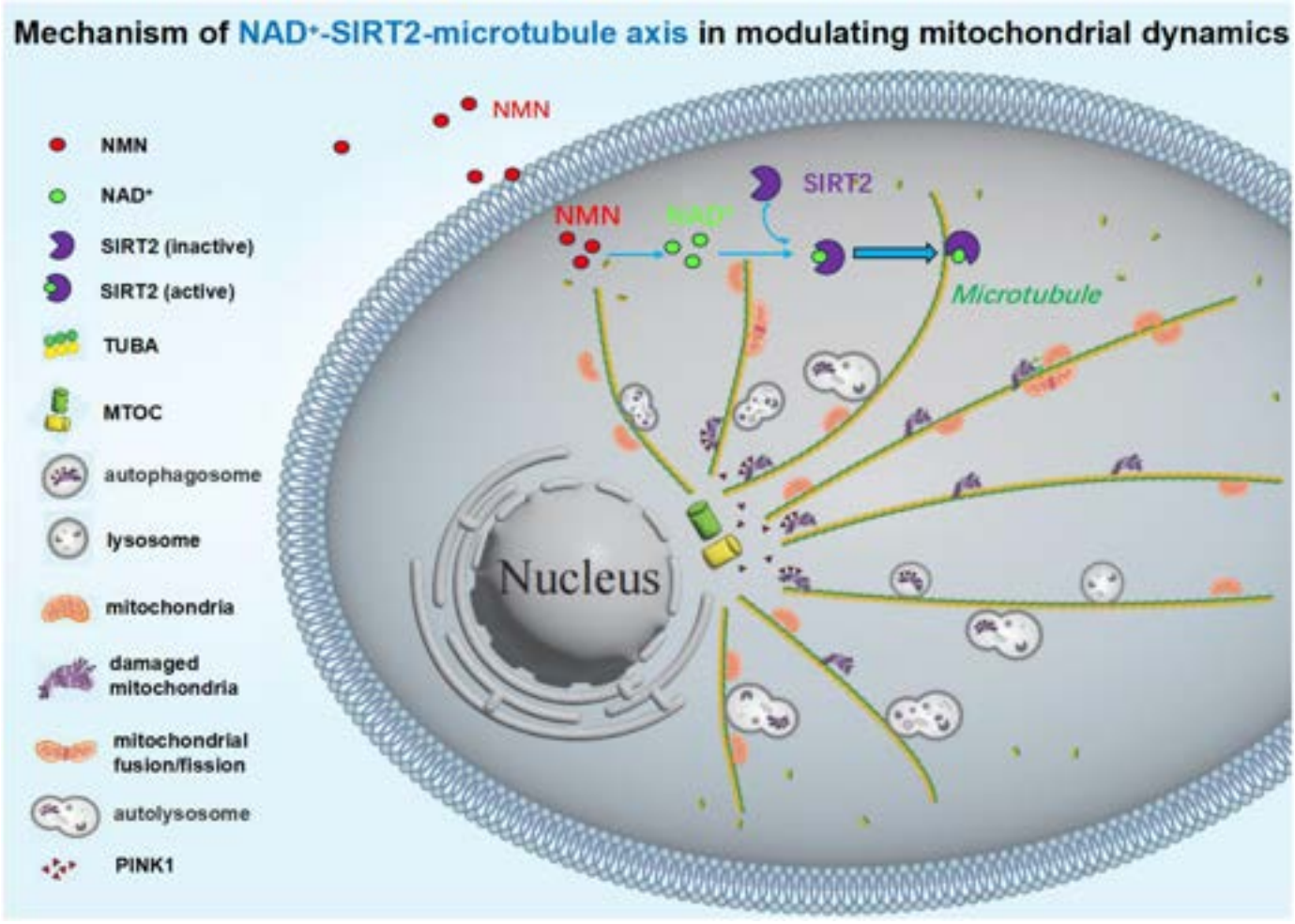

Figure 10. Potential mechanism of NAD^+-SIRT2-microtubule axis in modulating mitochondrial dynamics. Mitochondria, lysosome and autophagosome of damaged mitochondria are all intracellular membrane vesicles attached to and move along microtubules as trafficking tracks. Mitochondrial dynamics, including its movement, fusion/fission, and interaction with lysosome, is impaired in a senescent cell because of microtubule hyper-stabilization and declined microtubule dynamics, which however can be improved by NMN/NAD^+-induced elevation of SIRT2 activation (as a tubulin deacetylase) and microtubule dynamics.

Discussion

The profound impacts of NAD^+ on Sirtuins and Sirtuin-regulated functions have been well-documented, including SIRT1 and SIRT3-mediated improvements in mitochondrial function and energy metabolism [7,43]. While the potential effect of NAD^+ on SIRT2-regulated microtubule dynamics during aging or diseased conditions remain unexplored. Our results uncover a novel mechanism through which NAD^+ exerts the positive effect in improving mitochondrial homeostasis and function, which is relevant to SIRT2 activation-meditated microtubule destabilization and subsequently improved mitochondrial dynamics, as it is illustrated in Figure 10. This study provides new insights into the anti-aging effects of NMN/NAD^+ beyond its previously well-known roles. These findings also underscore the potential of NMN/NAD^+ as a therapeutic agent for age-related muscle degeneration.

Microtubule, key components of the cytoskeleton, plays a critical role in maintaining cellular structure and function. Importantly, microtubule serve as the trafficking track for various intracellular organelles and vesicles, and is crucial for modulating their distribution, movement, and interaction [45,46]. Microtubule is greatly involved in regulating mitochondrial dynamics such as mitochondrial movement, fission/fusion and interaction with autophagosome or lysosomal vesicles, as well as the process of mitophagy [47]. The dynamic instability of microtubule network (i.e., the polymerization and depolymerization process) is of particular importance for the kinetic activity of microtubule, which underlies their important biological functions [48]. Thus, proper microtubule dynamics is needed for smooth mitochondrial repair and mitophagy process. Hyper-stabilized microtubules are less dynamic and can impair cellular functions. In senescent cells, reduced SIRT2 activity can lead to hyper-acetylation of TUBA, increased microtubule stabilization and reduced microtubule dynamics. Reactivation of SIRT2 (e.g., by NMN supplementation) can restore TUBA deacetylation, destabilize microtubules, restore microtubule dynamics and improve cellular function, thereby delaying senescence.

SIRT2 is a mainly cytoplasmic localized protein, and can function as a tubulin deacetylase. SIRT2 plays a critical role in maintaining microtubule dynamics by deacetylating tubulin

[49,50]. Reduced SIRT2 activity in a cell can lead to hyper-acetylation of TUBA and increased microtubule stabilization. Microtubule hyper-stabilization results in reduced microtubule dynamics, which impairs microtubule-dependent mitochondrial dynamics (i.e., mitochondrial movement, fission and fusion, repair and mitophagy-dependent clearance), contributing to the senescent phenotype. Our findings demonstrate that SIRT2 inactivation is a key reason leading to the increased microtubule hyper-stabilization in senescent muscle cells. NMN, as a precursor of NAD^+, was effective in re-activating SIRT2 in senescent muscle cells. By boosting NAD^+ levels, NMN enhanced SIRT2 activity, leading to the deacetylation of TUBA and the restoration of microtubule dynamics [51]. Our results demonstrate that NMN treatment effectively repressed microtubule stabilization and delayed cellular senescence in muscle cells. It is notable that we also observed that NMN still exhibited partial effects after SIRT2 inhibition via siRNA in senescent cells, suggesting that other sirtuins such as SIRT1 and SIRT3, which are also NAD^+-dependent protein deacetylase, might have been activated by NMN through a mechanism of functional compensation, potentially assuming or overlapping with some of SIRT2's roles. Thus, in addition to SIRT2-microtubule axis, there are other parallel pathways in responding to NMN in senescent cells. These findings suggest that NMN supplementation could be a potential therapeutic strategy for age-related muscle degeneration. Therapeutic strategies targeting TUBA deacetylases, such as SIRT2 and HDAC6, may hold great promise for treating age-related conditions, neurodegenerative diseases, and other disorders associated with microtubule dysfunction.

In conclusion, our study demonstrates that NMN delayed muscle cell senescence by activating SIRT2-mediated microtubule destabilization, which revealed a novel mechanism for effective anti-aging strategies. These findings provide new insights into the role of SIRT2 in regulating microtubule dynamics during cellular senescence, and in mediating the anti-aging effect of NMN for age-related muscle cell defects. Microtubule-targeting methods may hold great therapeutic potential for addressing age-related muscle degeneration and sarcopenia disease.

Materials and methods

Cell source

Human primary skeletal muscle cells were ordered from ATCC (HSkMC; PCS-950–010) and Procell Life Science&Technology Co., Ltd. (HSkMC; CP-H095), and cultured in DMEM (Vivacell Biotechnology, C3103-0500) supplemented with 20% FBS. These HSkMCs were verified to be mostly muscle-derived mesenchymal stem/stromal cells (MSCs) with flow cytometry assay for MSC markers (positive for ENG/CD105, NT5E/CD73, and THY1/CD90, and negative for PTPRC/CD45), and immunostaining assay for PDGFRA (a marker for FAPs, a main subgroup of muscle MSCs) [52]. Mouse primary muscle cells were isolated from the gastrocnemius skeletal muscle of 2- or 18-month-old mice (Pengyue Experimental Animal Breeding Co., Ltd, SYXK(LU) 2024 0019) based on their quick adhering capacity to collagen-coated surface/substrate, and then sorted with fluorescence activated cell sorting (FACS) according to the positive expression of PDGFRA [29].

Induction of cellular senescence

Muscle cells were induced to senesce using D-galactose (D-gal), a well-established model for inducing oxidative stress and cellular senescence [53]. After 3 days of exposure, senescent cells were characterized by increased expression of senescence-associated markers, such as CDKN2A, CDKN1A and SASPs, and reduced proliferative capacity. And the senescent cells in skeletal muscle MSCs were also identified using the senescence-associated β-galactosidase (SA-GLB1/β-gal) Staining Kit (Cell Signaling Technology, 9860S) following the manufacturer's protocol. The number of cells positive for SA-GLB1/β-Gal activity at pH 6, a known characteristic of senescent cells, was determined.

Assessment of microtubule dynamics

Microtubule dynamics were assessed using live-cell imaging and immunofluorescence staining (Beyotime Biotechnology Co., Ltd., C2213S). The microtubule network images were transferred to gray and analyzed with ImageJ Tubeness plugin, which filters the images to show the "tube-like" points and structure in the image. Tubeness images were then analyzed with mitochondrial network analysis (MiNA) toolset plugin from ImageJ to check structural changes of microtubule [49]. The levels of acetylated TUBA/tubulin, a marker of microtubule stabilization, were measured using western blot analysis and immunofluorescence staining.

SIRT2 activity assay

SIRT2 activity was measured using a fluorometric assay that quantifies the deacetylation of a synthetic substrate. The levels of SIRT2 expression were assessed using western blot analysis. SIRT2 activation is achieved by overexpressing plasmids. We used pcDNA3.1-SIRT2-EGFP synthesized by GenePharma (Shanghai, China). *SIRT2* siRNA plasmid purchased from Santa Cruz Biotechnology (sc-40988) were used to repress the expression of SIRT2. In short, Human muscle cells were transfected with the pcDNA3.1-SIRT2-EGFP plasmid or *SIRT2* siRNA plasmid using jetPRIME transfection reagent (PolyPlus, 101,000,046) [54]. According to the manufacturer's instructions, when MSCs grew to 70–80% confluence, the cells were transfected with *SIRT2* overexpression plasmid (2 μg) or *SIRT2* targeted siRNA (2 μg) diluted in 200 μL jetPRIME® buffer. Then, add 4 μL of jetPRIME® reagent and incubate at room temperature for 10 min. At 12 h of transfection, the medium was replaced with DMEM medium containing 10% FBS to stop transfection. Stably transfected cells were selected by G418 medium (500 μg/mL, Shandong Sparkjade Biotechnology Co., Ltd., SJ-MA0055) [55].

NMN treatment

Senescent muscle cells were treated with NMN (Selleck, S5259) at various concentrations for 3 days. The effects of

NMN on SIRT2 activity, microtubule dynamics, mitophagy and cellular senescence were evaluated.

Mitochondrial function analysis

Cell mitochondrial membrane potential and active oxygen was detected using JC-1 Dye and MitoSOX Red (Invitrogen, M36008) [56,57]. Mitochondrial dynamics were assessed using live-cell imaging and immunofluorescence staining. Then, we used the mitochondrial network analysis (MiNA) toolset from ImageJ to semi-automatically analyze mitochondrial networks [58]. Using this plugin, we analyzed and compared changes in mitochondrial branches, including branches, branch length, and branch junctions. In addition, the leakage of mtDNA was detected by immunofluorescence staining through the colocalization between TFAM and TOMM20.

Mitophagy Analysis

Fluorescent probes were used to stain lysosomes on mitophagy according to manufacturer's instructions: LysoTracker™ Deep Red (Invitrogen, L12492) [59]. Then, mitophagy related-protein levels, such as PRKN, PINK1, and LAMP1 were assessed using western blot or immunofluorescence staining.

Direct detection of mitophagy

Mitophagy was also detected using the Mitophagy Detection Kit including Mtphagy Dye and Lyso Dye (Dojindo Molecular Technologies, MT02) [44]. In brief, cells were first washed twice with HBSS (Solarbio, H1040-500), followed by incubation at 37°C for 30 min with DMEM containing 100 nmol Mtphagy Dye. After incubation, the cells were washed twice again with HBSS, then further incubated for 30 min with 1 μM Lyso Dye and Hoechst. After two additional washes with HBSS, the cells were observed using fluorescence microscopy [60].

Western blot

Protein samples from MSCs were subjected to SDS-PAGE and transferred to PVDF membranes. BSA (5%; Beijing labgic Co., Ltd., BS114) was then added to seal the PVDF membranes for 1 h at room temperature. The PVDF membranes were washed three times using TBST (10 min each time; Shandong Sparkjade Biotechnology Co., Ltd., ED0010). The primary antibodies used were acetyl-TUBA/α-tubulin (Abcam, EPR16772), TUBA (Abcam, EP1332Y), CDKN2A/p16 (Santa Cruz Biotechnology, sc-1661), CDKN1A/p21 (Santa Cruz Biotechnology, sc-471), PRKN/Parkin (Santa Cruz Biotechnology, sc-32282), PINK1 (Santa Cruz Biotechnology, sc-517353), CGAS (Santa Cruz Biotechnology, sc-515777), STING1 (Cell Signaling Technology, 13,647), p-STING1 (Cell Signaling Technology, 50,907), TFAM (Santa Cruz Biotechnology, sc-166965), TOMM20 (Abcam, EPR15581-54), and LAMP1 (Santa Cruz Biotechnology, sc-20011), GAPDH(Abcam, EPR16891) were all applied at a 1:100 to 1:1000 dilution. Diluted primary antibody was added and incubated at 4°C for 16 h. After the PVDF membranes were washed, horseradish peroxidase-labeled secondary antibody (Proteintech, SA00001) working solution was added and incubated at 37°C for 60 min. The secondary antibody was discarded, and the membranes were washed three times using TBST (10 min each time). ECL (enhanced chemiluminescence; Proteintech, PK10002) was added to detect immune protein bands. Blots were imaged with the iBright™ CL750 Imaging system (Thermo Scientific, USA). The band intensities were measured using Image software (version 1.48, National Institutes of Health, Bethesda, MD, USA) and normalized to those of GAPDH (loading control). The original immunoblot images corresponding to the western blot results shown in the figures are provided in Data S1.

PCR analysis

mRNA analysis via reverse transcriptase-PCR: Total RNA was obtained from MSCs using the RNeasy Mini Kit (Qiagen, 74,104) according to the manufacturer's instructions. Reverse transcription was performed using an iScript cDNA Synthesis Kit (Bio-Rad Laboratories, 1725035BUN). Quantitative real-time PCR was performed using an iCycler thermal cycler (Bio-Rad Laboratories, USA). The gene-specific primer sequences used are listed in Table S1 for *CDKN2A*, *CDKN1A*, *CDKN1B/p27*, *MMP1*, *IL1A/IL-1α*, *IL1B/1 L-1β*, *IL6*, *CXCL1*, *IFNA/IFN-α*, *IFNB/IFN-β* and *GAPDH*, which was used as an internal control to normalize gene expression. The cycling parameters used for all primers were as follows: 95°C for 10 min; PCR, 40 cycles of 30 s at 95°C for denaturation, 1 min at 54°C for annealing and 30 s at 72°C for extension. All data were normalized to the expression of *GAPDH*.

SIRT2 activity detection with Elisa

After collecting cell lysates, add 100 μL of standards (0, 62.5, 125, 250, 500, 1000, 2000, 4000 pg/mL) from the SIRT2 ELISA kit (Abcam, ab227895) [61,62] and test samples to the plate wells. Seal the plate and incubate at 37°C for 50 min. After incubation, discard the liquid and wash each well with 300 μL of wash buffer, allowing it to stand for 30 seconds before removal. Repeat this washing procedure three times. Then add 100 μL of biotinylated antibody working solution to each well and incubate at 37°C for 50 min. Perform the washing procedure as described above, then add 100 μL of SMAC complex solution to each well and incubate at 37°C for 50 min. After repeating the washing procedure as before, add 100 μL of TMB mixture to each well, mix thoroughly, and incubate in the dark at 37°C for 10–20 min until blue color develops. Finally, add 50 μL of stop solution to each well to terminate the reaction, and immediately measure the optical density at 450 nm using a microplate reader.

Plasmid transfection to overexpress SIRT2

pcDNA3.1-SIRT2-EGFP were synthesized by GenePharma (Shanghai, China). The target gene was *Homo sapiens SIRT2* (sirtuin 2), transcript variant 1 mRNA, NCBI Reference Sequence: NM_012237.4. Human muscle cells were transfected with the pcDNA3.1-SIRT2-EGFP plasmid using jetPRIME transfection reagent. At 4 h of transfection, the

medium was replaced with DMEM medium containing 10% FBS to stop transfection. Stably transfected cells were selected using G418 medium.

Modulation of microtubule stability

Microtubule-stabilizing drug paclitaxel (5 nM for 2 days; Selleck, S1150) and the SIRT2-specific inhibitor SirReal2 (10 μM for 2 days; Shandong Sparkjade Biotechnology Co., Ltd., SJ-MX4665) were applied treat MSCs to simulate the effects of NP-induced microtubule stabilization; colchicine treatment (2 nM for 2 days; Selleck, S2284) of MSCs was applied to transiently destabilize microtubule.

5-ethynyl-20-deoxyuridine (EdU) staining

Cell proliferation was detected using Click-iT EdU Imaging Systems (Invitrogen, C10337). Briefly, MSCs were incubated with EdU for 30 min, fixed in 1:1 acetone:methanol or 4% paraformaldehyde (PFA), and incubated with a Click-iT EdU reaction cocktail for 30 min. Cell nucleus was stained with DNA binding reagent 4′,6-diamidino-2-phenylindole (DAPI) for 5 min. Finally, cells were examined using a Nikon TE 2000 microscope (Nikon, Tokyo, Japan).*Microtubule Polymerization Assay by Turbidity Measurement*

The microtubule polymerization status was analyzed using a turbidity assay, performed according to previously described methods with appropriate modifications [63]. Briefly, approximately 1×10^6 cells were collected and resuspended in microtubule-stabilizing buffer (containing 100 mM PIPES, 1 mM EGTA, 1 mM $MgCl_2$, pH 6.9) supplemented with 10 μM paclitaxel to stabilize polymerized microtubules and protease inhibitor cocktail (Beyotime Biotechnology Co., Ltd., P1008) to prevent protein degradation. The cell suspension was subjected to ultrasonication (80 W power, 5 s pulses with 10 s intervals, repeated 5 times) to thoroughly disrupt cell membranes. The lysate was then centrifuged at 10,000 × g for 10 min at 37°C to remove cellular debris and unbroken cells. The supernatant was collected and further centrifuged at 100,000 × g for 30 min at 37°C to separate microtubule polymers from soluble proteins. The pellet, containing polymerized microtubules, was resuspended in the same buffer and immediately subjected to absorbance measurement at 340 nm (OD_{340}) using a spectrophotometer to evaluate the degree of microtubule polymerization.

Statistical analysis

Image analysis was performed using ImageJ software (version 1.48; National Institutes of Health, Bethesda, MD, USA). Data from at least six groups of samples (i.e., 6 visions of imaging) were pooled for statistical analysis, with at least three biological replicates and two technical replicates. Prism software (GraphPad) was used to plot graphs and the results were given as the mean ± standard deviation (SD). The statistical significance of any difference was calculated using Student's t test. p values < 0.05 were considered statistically significant.

Acknowledgements

We greatly appreciate the support from School of Pharmaceutical Sciences, National Key Laboratory of Advanced Drug Delivery System, Joint Innovation Team for Clinical & Basic Research (program 202401), Shandong First Medical University & Shandong Academy of Medical Sciences; and support from Shandong Cancer Hospital and Institute, Shandong First Medical University and Shandong Academy of Medical Science.

Author contributions

CRediT: **Jie Cui:** Conceptualization, Formal analysis, Investigation, Methodology; **Shifeng Ren:** Conceptualization, Formal analysis, Investigation, Methodology; **Bingjie Wang:** Conceptualization, Formal analysis, Investigation, Methodology; **Nan Zhang:** Investigation, Methodology; **Shanshan Zhu:** Investigation, Methodology; **Yajun Zhang:** Formal analysis, Investigation; **Xiangqing Qi:** Investigation; **Weixue Meng:** Investigation; **Liwei Shao:** Project administration, Writing – original draft; **Shan Gao:** Project administration, Writing – original draft; **Lijie Xing:** Supervision, Writing – original draft, Writing – review & editing; **Zengjun Li:** Resources, Supervision, Writing – original draft, Writing – review & editing; **Xiaodong Mu:** Conceptualization, Funding acquisition, Supervision, Writing – original draft, Writing – review & editing.

Funding

Funding to Xiaodong Mu: grant number [ZR2022MC025] from Natural Science Foundation of Shandong Province. Funding to Lijie Xing: grant number [tsqn202312361] from Taishan Scholar Foundation of Shandong Province, and grant number [ZR2025QA21] from Science Fund for Distinguished Young Scholars of Shandong Province.

Disclosure statement

No potential conflict of interest was reported by the author(s).

Data availability statement

The datasets generated during the current study are available from the corresponding author on reasonable request.

References

[1] Covarrubias AJ, Perrone R, Grozio A, et al. NAD(+) metabolism and its roles in cellular processes during ageing. Nat Rev Mol Cell Biol. 2021;22(2):119–141. doi: 10.1038/s41580-020-00313-x
[2] Chu X, Raju RP. Regulation of NAD(+) metabolism in aging and disease. Metabolism. 2022;126:154923. doi: 10.1016/j.metabol.2021.154923
[3] Soma M, Lalam SK. The role of nicotinamide mononucleotide (NMN) in anti-aging, longevity, and its potential for treating chronic conditions. Mol Biol Rep. 2022;49(10):9737–9748. doi: 10.1007/s11033-022-07459-1
[4] Yoshino J, Baur JA, Imai SI. NAD(+) intermediates: the biology and therapeutic potential of NMN and nr. Cell Metab. 2018;27(3):513–528.
[5] Imai S, Guarente L. NAD+ and sirtuins in aging and disease. Trends Cell Biol. 2014;24(8):464–471. doi: 10.1016/j.tcb.2014.04.002
[6] Rahman SU, Qadeer A, Wu Z. Role and potential mechanisms of nicotinamide mononucleotide in aging. Aging Dis. 2024;15(2):565–583. doi: 10.14336/AD.2023.0519-1
[7] Kane AE, Sinclair DA. Sirtuins and NAD(+) in the development and treatment of metabolic and cardiovascular diseases. Circ Res. 2018;123(7):868–885. doi: 10.1161/CIRCRESAHA.118.312498

[8] Ding YN, Wang HY, Chen XF, et al. Roles of sirtuins in cardiovascular diseases: mechanisms and therapeutics. Circ Res. 2025;136(5):524–550. doi: 10.1161/CIRCRESAHA.124.325440
[9] Liu Y, Zhang Y, Zhu K, et al. Emerging role of sirtuin 2 in Parkinson's disease. Front Aging Neurosci. 2019;11:372.
[10] Cha Y, Kim T, Jeon J, et al. SIRT2 regulates mitochondrial dynamics and reprogramming via MEK1-ERK-DRP1 and AKT1-DRP1 axes. Cell Rep. 2021;37(13):110155. doi: 10.1016/j.celrep.2021.110155
[11] Naren P, Samim KS, Tryphena KP, et al. Microtubule acetylation dyshomeostasis in Parkinson's disease. Transl Neurodegener. 2023;12(1):20. doi: 10.1186/s40035-023-00354-0
[12] Zheng C, Li Y, Wu X, et al. Advances in the synthesis and physiological metabolic regulation of nicotinamide mononucleotide. Nutrients. 2024;16(14):2354. doi: 10.3390/nu16142354
[13] Wang H, Sun Y, Pi C, et al. Nicotinamide mononucleotide supplementation improves mitochondrial dysfunction and rescues cellular senescence by NAD(+)/Sirt3 pathway in mesenchymal stem cells. Int J Mol Sci. 2022;23(23):14739. doi: 10.3390/ijms232314739
[14] De Belly H, Paluch EK, Chalut KJ. Interplay between mechanics and signalling in regulating cell fate. Nat Rev Mol Cell Biol. 2022;23(7):465–480. doi: 10.1038/s41580-022-00472-z
[15] Moujaber O, Stochaj U. The cytoskeleton as regulator of Cell signaling pathways. Trends Biochem Sci. 2020;45(2):96–107. doi: 10.1016/j.tibs.2019.11.003
[16] Ruiz-Zapata AM, Heinz A, Kerkhof MH, et al. Extracellular matrix stiffness and composition regulate the myofibroblast differentiation of vaginal fibroblasts. Int J Mol Sci. 2020;21(13):4762. doi: 10.3390/ijms21134762
[17] Mohan N, Sorokina EM, Verdeny IV, et al. Detyrosinated microtubules spatially constrain lysosomes facilitating lysosome-autophagosome fusion. J Cell Biol. 2019;218(2):632–643.
[18] Yue X, Cui J, Sun Z, et al. Nuclear softening mediated by Sun2 suppression delays mechanical stress-induced cellular senescence. Cell Death Discov. 2023;9(1):167. doi: 10.1038/s41420-023-01467-1
[19] Cohen S, Valm AM, Lippincott-Schwartz J. Interacting organelles. Curr Opin Cell Biol. 2018;53:84–91. doi: 10.1016/j.ceb.2018.06.003
[20] Jahreiss L, Menzies FM, Rubinsztein DC. The itinerary of autophagosomes: from peripheral formation to kiss-and-run fusion with lysosomes. Traffic. 2008;9(4):574–587. doi: 10.1111/j.1600-0854.2008.00701.x
[21] Nakatogawa H. Mechanisms governing autophagosome biogenesis. Nat Rev Mol Cell Biol. 2020;21(8):439–458. doi: 10.1038/s41580-020-0241-0
[22] Moore AS, Holzbaur ELF. Mitochondrial-cytoskeletal interactions: dynamic associations that facilitate network function and remodeling. Curr Opin Physiol. 2018;3:94–100. doi: 10.1016/j.cophys.2018.03.003
[23] Longuet M, Serduc R, Riva C. Implication of bax in apoptosis depends on microtubule network mobility. Int J Oncol. 2004;25(2):309–317. doi: 10.3892/ijo.25.2.309
[24] Brouhard GJ, Rice LM. Microtubule dynamics: an interplay of biochemistry and mechanics. Nat Rev Mol Cell Biol. 2018;19(7):451–463. doi: 10.1038/s41580-018-0009-y
[25] Chu S, Moujaber O, Lemay S, et al. Multiple pathways promote microtubule stabilization in senescent intestinal epithelial cells. NPJ Aging. 2022;8(1):16. doi: 10.1038/s41514-022-00097-8
[26] Chan A, Gilfillan C, Templeton N, et al. Induction of accelerated senescence by the microtubule-stabilizing agent peloruside a. Invest New Drugs. 2017;35(6):706–717. doi: 10.1007/s10637-017-0493-5
[27] Wu Y, Wu Y, Yang Y, et al. Lysyl oxidase-like 2 inhibitor rescues D-galactose-induced skeletal muscle fibrosis. Aging Cell. 2022;21(7):e13659. doi: 10.1111/acel.13659
[28] Chen M, Huang X, Li B, et al. ArfGAP3 protects mitochondrial function and promotes autophagy through Rab5a-mediated signals in ageing skeletal muscle. J Cachexia Sarcopenia Muscle. 2025;16(1):e13725. doi: 10.1002/jcsm.13725
[29] Mu X, Tseng C, Hambright WS, et al. Cytoskeleton stiffness regulates cellular senescence and innate immune response in Hutchinson-Gilford progeria syndrome. Aging Cell. 2020;19(8):e13152. doi: 10.1111/acel.13152
[30] Colin A, Singaravelu P, Théry M, et al. Actin-network architecture regulates microtubule dynamics. Curr Biol. 2018;28(16):2647–2656.e2644.
[31] Uchida K, Scarborough EA, Prosser BL. Cardiomyocyte microtubules: control of mechanics, transport, and remodeling. Annu Rev Physiol. 2022;84(1):257–283. doi: 10.1146/annurev-physiol-062421-040656
[32] Gadadhar S, Bodakuntla S, Natarajan K, et al. The tubulin code at a glance. J Cell Sci. 2017;130(8):1347–1353. doi: 10.1242/jcs.199471
[33] Moujaber O, Fishbein F, Omran N, et al. Cellular senescence is associated with reorganization of the microtubule cytoskeleton. Cell Mol Life Sci. 2019;76(6):1169–1183. doi: 10.1007/s00018-018-2999-1
[34] Caporizzo MA, Prosser BL. The microtubule cytoskeleton in cardiac mechanics and heart failure. Nat Rev Cardiol. 2022;19(6):364–378. doi: 10.1038/s41569-022-00692-y
[35] Shi X, Jiang X, Chen C, et al. The interconnections between the microtubules and mitochondrial networks in cardiocerebrovascular diseases: implications for therapy. Pharmacol Res. 2022;184:106452. doi: 10.1016/j.phrs.2022.106452
[36] Vona R, Mileo AM, Matarrese P. Microtubule-based mitochondrial dynamics as a valuable therapeutic target in Cancer. Cancers (Basel). 2021;13(22):5812. doi: 10.3390/cancers13225812
[37] Zhou H, Khan D, Hussain SM, et al. Colchicine prevents oxidative stress-induced endothelial cell senescence via blocking NF-κB and MAPKs: implications in vascular diseases. J Inflamm (Lond). 2023;20(1):41. doi: 10.1186/s12950-023-00366-7
[38] Dalbeth N, Lauterio TJ, Wolfe HR. Mechanism of action of colchicine in the treatment of gout. Clin Ther. 2014;36(10):1465–1479. doi: 10.1016/j.clinthera.2014.07.017
[39] Peng Y, Li Z, Zhang J, et al. Low-dose colchicine ameliorates doxorubicin cardiotoxicity via promoting autolysosome degradation. J Am Heart Assoc. 2024;13(9):e033700. doi: 10.1161/JAHA.123.033700
[40] Kim J, Kim HS, Chung JH. Molecular mechanisms of mitochondrial DNA release and activation of the cGAS-STING pathway. Exp Mol Med. 2023;55(3):510–519. doi: 10.1038/s12276-023-00965-7
[41] Li Y, Cui J, Liu L, et al. mtDNA release promotes cGAS-STING activation and accelerated aging of postmitotic muscle cells. Cell Death Dis. 2024;15(7):523. doi: 10.1038/s41419-024-06863-8
[42] Liu H, Zhen C, Xie J, et al. TFAM is an autophagy receptor that limits inflammation by binding to cytoplasmic mitochondrial DNA. Nat Cell Biol. 2024;26(6):878–891. doi: 10.1038/s41556-024-01419-6
[43] Gudimchuk NB, McIntosh JR. Regulation of microtubule dynamics, mechanics and function through the growing tip. Nat Rev Mol Cell Biol. 2021;22(12):777–795. doi: 10.1038/s41580-021-00399-x
[44] Kameyama K, Motoyama K, Tanaka N, et al. Induction of mitophagy-mediated antitumor activity with folate-appended methyl-β-cyclodextrin. Int J Nanomed. 2017;12:3433–3446.
[45] de Forges H, Bouissou A, Perez F. Interplay between microtubule dynamics and intracellular organization. Int J Biochem Cell Biol. 2012;44(2):266–274. doi: 10.1016/j.biocel.2011.11.009
[46] Nambiar A, Manjithaya R. Driving autophagy - the role of molecular motors. J Cell Sci. 2024;137(3).jcs260481. doi:10.1242/jcs.260481

[47] Schmitt K, Grimm A, Dallmann R, et al. Circadian control of DRP1 activity regulates mitochondrial dynamics and bioenergetics. Cell Metab. 2018;27(3):657–666.e655.
[48] Gardner MK, Zanic M, Howard J. Microtubule catastrophe and rescue. Curr Opin Cell Biol. 2013;25(1):14–22. doi: 10.1016/j.ceb.2012.09.006
[49] Inoue T, Hiratsuka M, Osaki M, et al. SIRT2, a tubulin deacetylase, acts to block the entry to chromosome condensation in response to mitotic stress. Oncogene. 2007;26(7):945–957. doi: 10.1038/sj.onc.1209857
[50] Eshun-Wilson L, Zhang R, Portran D, et al. Effects of α-tubulin acetylation on microtubule structure and stability. Proc Natl Acad Sci U S A. 2019;116(21):10366–10371. doi: 10.1073/pnas.1900441116
[51] Liang N, Liu S, Wang Y, et al. Nicotinamide mononucleotide (NMN) improves the senescence of mouse vascular smooth muscle cells induced by Ang ii through activating p-AMPK/KLF4 pathway. Pharmaceuticals (Basel). 2025;18(4):553. doi: 10.3390/ph18040553
[52] Cui J, Yue X, Zhang Y, et al. Polystyrene nanoplastics promote muscle cell senescence through microtubule hyper-stabilization-mediated mitophagy dysfunction and cGAS-sting activation. J Hazard Mater. 2025;496:139232. doi: 10.1016/j.jhazmat.2025.139232
[53] Azman KF, Zakaria R. D-Galactose-induced accelerated aging model: an overview. Biogerontology. 2019;20(6):763–782. doi: 10.1007/s10522-019-09837-y
[54] Li Y, Bie J, Song C, et al. SIRT2 negatively regulates the cGAS-STING pathway by deacetylating G3BP1. The EMBO Rep. 2023;24(12):e57500. doi: 10.15252/embr.202357500 *EMBO reports*.
[55] Gong H, Zheng C, Lyu X, et al. Inhibition of Sirt2 alleviates fibroblasts activation and pulmonary fibrosis via Smad2/3 pathway. Front Pharmacol. 2021;12:756131. doi: 10.3389/fphar.2021.756131
[56] Zhou R, Yazdi AS, Menu P, et al. A role for mitochondria in NLRP3 inflammasome activation. Nature. 2011;469(7329):221–225. doi: 10.1038/nature09663
[57] Xu D, Liu L, Zhao Y, et al. Melatonin protects mouse testes from palmitic acid-induced lipotoxicity by attenuating oxidative stress and DNA damage in a SIRT1-dependent manner. J Pineal Res. 2020;69(4):e12690. doi: 10.1111/jpi.12690
[58] Valente AJ, Maddalena LA, Robb EL, et al. A simple ImageJ macro tool for analyzing mitochondrial network morphology in mammalian cell culture. Acta Histochem. 2017;119(3):315–326. doi: 10.1016/j.acthis.2017.03.001
[59] Ordureau A, Paulo JA, Zhang J, et al. Global landscape and dynamics of Parkin and USP30-dependent ubiquitylomes in iNeurons during mitophagic signaling. Mol Cell. 2020;77(5):1124–1142.e1110. doi: 10.1016/j.molcel.2019.11.013
[60] König J, Ott C, Hugo M, et al. Mitochondrial contribution to lipofuscin formation. Redox Biol. 2017;11:673–681. doi: 10.1016/j.redox.2017.01.017
[61] Sola-Sevilla N, Mesa-Lombardo A, Aleixo M, et al. SIRT2 inhibition rescues neurodegenerative pathology but increases systemic inflammation in a transgenic mouse model of Alzheimer's disease. J Neuroimmune Pharmacol. 2023;18(3):529–550. doi: 10.1007/s11481-023-10084-9
[62] Lu W, Hou D, Chen X, et al. Elevated SIRT2 of serum exosomes is positively correlated with diagnosis of acute ischemic stroke patients. BMC Neurol. 2023;23(1):321. doi: 10.1186/s12883-023-03348-7
[63] Mirigian M, Mukherjee K, Bane SL, et al. Measurement of in vitro microtubule polymerization by turbidity and fluorescence. Methods Cell Biol. 2013;115:215–229 doi:10.1016/B978-0-12-407757-7.00014-1.